Wave-based sensor responses with embedded electrode layouts

Rishikesh Srinivasaraghavan Govindarajan^a, Foram Madiyar^b, Daewon Kim*^a

Dept. of Aerospace Engineering; ^bDept. of Physical Science;

Embry-Riddle Aeronautical University, 1 Aerospace Blvd., Daytona Beach, FL, USA 32114

ABSTRACT

Acoustic wave-based devices have attracted greater attention, particularly in the aerospace and bio-medical fields due to their passive and wireless capabilities. Interdigital transducer (IDT) is an integral part of the SHM wave-based sensor, as it transmits information about the structural state. Additionally, embedding the electrodes inside the piezoelectric substrate increases the acoustic coupling and protects the electrodes from potential external damage. This paper uses numerical analysis to discuss sensor responses with different IDT layouts in both frequency and time domains. The results investigate each type's sensitivity towards mechanical strains and figure of merit, which facilitates the development of an efficient embedded electrode sensor through advanced additive manufacturing techniques.

Keywords: IDT layouts, piezoelectric, embedded electrodes

1. INTRODUCTION

Acoustic wave-based piezoelectric sensors have emerged over the decades in multiple disciplines as an ideal candidate for structural health monitoring (SHM) methods because of their adjustable frequency range, easy processability, and wireless capability¹⁻⁴. Evaluation of strain concentrations during the additive manufacturing process demands a micro-sized sensor that can detect meaningful information wirelessly to ensure quality. Piezoelectric substrate (related to wave velocity) and interdigital transducer (IDT) electrodes (related to frequency response) are the significant parts of the acoustic wave-based sensors. For an effective sensor, IDT design must be designed well as they play a vital role in dictating frequency response, output signal characteristics, and generated wave patterns. The basic constitutive piezoelectric equation for strain or electric displacement measurement in the material is given by,

$$S = sT + d^t E (1)$$

$$D = dT + \varepsilon E \tag{2}$$

where S, T, E, and D are the strain, stress, electric field, and electric charge density displacement components, respectively. The piezoelectric strain coefficient d, the elastic compliance s, and dielectric constant ε are associated with mechanical strains⁵. Maxwell's equation and equation of motion, along with piezoelectric coupled equations (1) and (2) are solved together to form a solution for acoustic wave-based problems. Selecting an appropriate IDT layout with high sensitivity is critical in developing an acoustic sensor.

Polyvinylidene fluoride (PVDF), a well-known stable polymer exhibiting flexibility and piezoelectric properties, is selected as a substrate material. Different IDT layouts have been explored for multidisciplinary projects⁶⁻¹¹; however, a better interpretation of sensor behavior exhibiting different IDT layouts embedded inside the substrate has not yet been explored to understand the efficiency towards mechanical strain sensitivity. This paper aims to investigate the performance of a two-port piezoelectric sensor with different embedded electrode layouts, as shown in Figure 1 (a). The numerical analysis includes scattering parameter and voltage response in frequency and time domains. Compared to the surface deposited IDTs, embedding the electrode demonstrates an enhancement in sensitivity due to higher piezoelectric coupling¹²⁻¹⁴, which also protects the IDT structure from the external environment. The sensitivity of each IDT layout towards mechanical strains is quantified using an initial strain model with varying mechanical strain concentrations. The effectiveness of each layout type is decided based on the sensitivity, coupling (k²), and quality factors (Q). Based on the

^{*}kimd3c@erau.edu; phone 1-386-226-7262; ERAU SMART lab

investigated results, a high-performance sensor with a unique IDT design can be developed by combining the benefits of each type through advanced additive manufacturing techniques that expand the range of applications.

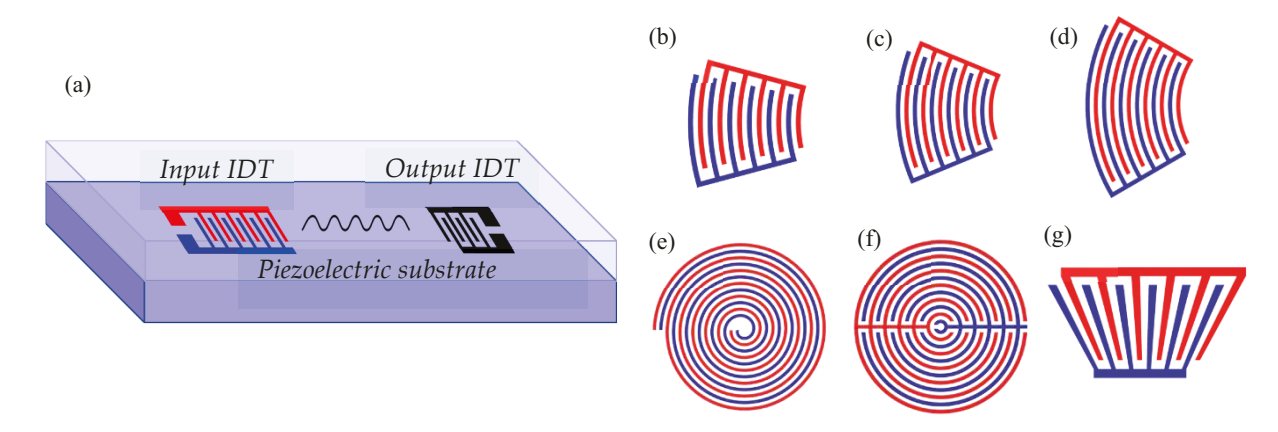


Figure 1. (a) Schematic of a two-port piezoelectric sensor with electrodes embedded in the middle of the substrate (the upper half of substrate is transparent to show the electrode location); different IDT layouts studied in this work - FIDTs degree of arc (b) 30°, (c) 45°, (d) 60°; circular pattern (e) spiral, (f) holographic; and (g) slanted.

2. NUMERICAL MODELING OF PIEZOELECTRIC SENSOR

The primary goal of the acoustic sensor with embedded electrodes is to be sensitive to the applied mechanical strain exhibiting better coupling and figure of merits. To validate the piezoelectric sensor's performance with different IDT layouts embedded inside the substrate, the sensor behavior, particularly the scattering parameter and output voltage response, is analyzed in both frequency and time domains.

2.1 Different IDT layouts

The electrode design must be properly constructed to provide optimal sensor performance because several parameters predict the wave characteristics, such as wavelength, layout type, and delay line. IDT layouts such as focused, circular, and slanted designs are modeled for input IDTs, as shown in Figure 1 (b-g), to examine their performance with electrodes embedded inside the substrate. Output electrodes are fabricated of a bi-directional design, which receives the propagated acoustic waves. Focused IDT (FIDT) patterns on acoustic sensors are used mainly to generate waves with high intensity at a focused point. Their performance depends on the degree of arc, focal length, and spacing between IDTs. Among these, the frequency response is not affected by the change in focal length⁷, and operating frequency can be dictated based on the electrode spacing. The degree of arc has a crucial influence on the generated waves' focusing characteristics and is essential to identify the optimal degree of arc correlated towards device sensitivity through simulated data⁸. In this work, FIDT performance with 30°, 45° and 60° of arc with a 1.25 mm focal length is designed, simulated, and compared.

Furthermore, circular IDT designs with electrodes next to each other (spiral) and a holographic style are designed and simulated. The circular layout has the potential to generate waves in a larger area of the piezoelectric substrate and can be extended in multi-axial sensing. Lastly, the slanted type features a varying finger spacing across the electrode's length, enabling the sensor to operate in a wide frequency range¹. All the layouts are designed with a 2.5 mm delay line (distance between input and output electrodes), 50 µm spacing, 6 input pairs, 3 output pairs, and 0.5 metallization ratio.

2.2 Piezoelectric sensor setup

Finite element modeling allows appropriate optimization of components or layouts before fabrication in a convenient manner, particularly for complex 3-dimensional analysis. In this study, the simulations are based on PVDF substrate employed with the commercially available FEA tool COMSOL Multiphysics 6.0 package to analyze various layouts behavior by avoiding 2D infinite periodic structure approximation. COMSOL, a well-known tool for micro-MEMS

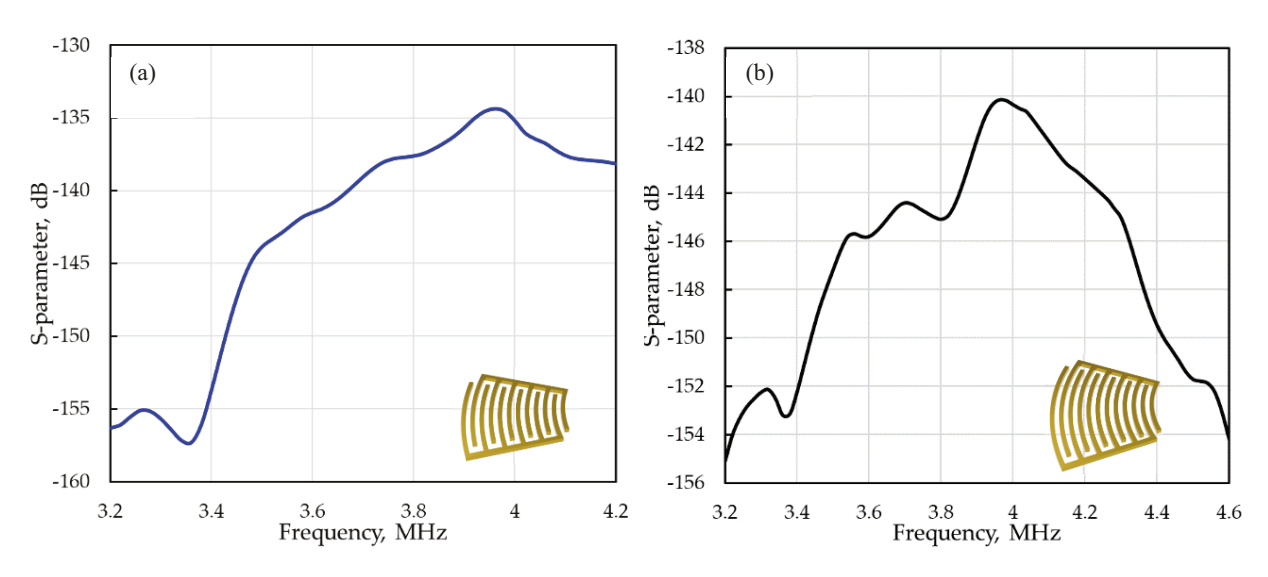
devices, considers mechanical, electrical, and piezoelectric properties with two physics: solid mechanics and electrostatics¹⁵. The material properties of substrate and electrodes made of PVDF and silver are assigned to respective domains. Major properties to be specified for a piezoelectric sensor are compliance matrix [s], dielectric constant [ϵ], and density [ρ], as listed in Table 1, along with polarization direction (default: z-direction). A 3D model with different IDT layouts embedded in the middle of the sensor's thickness direction is analyzed in both the time and frequency domains. The boundary conditions used during the simulation include a lower reflective boundary at the side walls to evade reflections and fixed constraints on the bottom surface. Overall domain with PVDF substrate and IDT layouts is meshed using a tetrahedral element with a size of $\lambda/8$ and $\lambda/4$, respectively.

Table 1. Material properties of the piezoelectric sensor.

Description	Value				
Polyvinylidene fluoride (PVDF)					
Density ρ [kg/m ³]	1,780				
Young's modulus E [GPa]	3				
Poisson's ratio v	0.3				
Elastic compliance matrix [10 ⁻¹⁰ . Pa ⁻¹]	$s_{11} = 3.781$ $s_{12} = -1.482$ $s_{13} = -1.724$ $s_{33} = 10.92$ $s_{44} = 14.28$ $s_{66} = 11.1$ $\varepsilon_{11} = 7.4$				
Dielectric constant	$ \epsilon_{22} = 9.3 $ $ \epsilon_{33} = 7.6 $				
Silver (Ag)					
Density ρ [kg/m ³]	10,500				
Young's modulus E [GPa]	83				
Poisson's ratio v	0.37				

2.3 Frequency domain study

A frequency domain analysis is studied to simulate the scattering parameter (S_{21}), which indicates the operational frequency of the specific design as a function of frequency. The terminated terminal feature is utilized in COMSOL to evaluate the S-parameter represented in dB with a reference 50 Ω impedance. An input power of 10 mW, equivalent to 10 dBm, is applied to the input electrode based on the experimental VNA measurement.



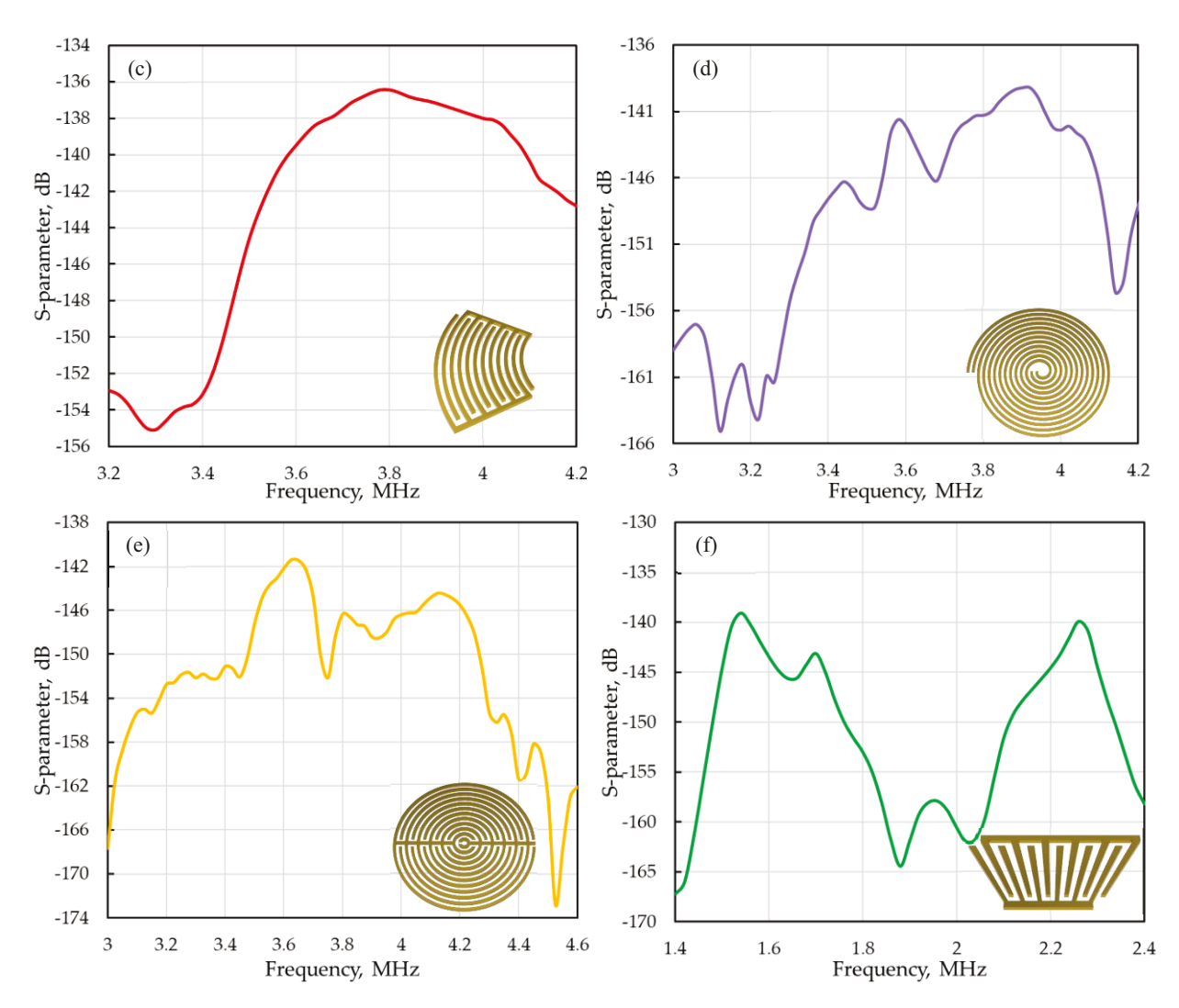


Figure 2. Scattering parameter (S_{21}) response as a function of frequency for different IDT layouts: FIDTs degree of arc (a) 30°, (b) 45°, (c) 60°; circular pattern (d) spiral, (e) holographic; and (f) slanted with 100 μ m spacing.

The obtained response for each layout case is measured in dB, representing the magnitude of power loss on the signal traveling between the input and output electrodes. Figure 2 (a-f) shows the distinct response for each electrode type, and for a slanted type, the frequency peak response for 100 µm is displayed among multiple resonant peaks.

2.4 Time domain study

To study the amplitude of voltage response from the output electrode, the time domain is executed using a transient analysis with an input sinusoidal response at the resonant frequency and a magnitude of 1V lasting 18 cycles (time depends on the resonant frequency of each layout). The voltage signal is applied to the input IDT using the voltage terminal feature to evaluate the voltage response as a function of time. Different wave modes are generated with the input voltage and will be separated after traveling a specified distance due to the traveling velocity difference. The voltage amplitude is obtained from the output positive for a specific wave mode, which converts the received mechanical waves into a voltage response. The scattering parameter and output signal response are summarized in Table 2. Among the different layouts, FIDT with 45° degree of arc and spiral showcases a higher output signal along with better scattering characteristics. In general, too large or smaller degree of arc shows an unfocused or unstable response 16, which supports the response attained through the simulation for FIDT layout. The slanted design shows a range of resonant peaks desirable for a wide frequency operation and is still the same as the bi-directional design, where the waves are dispersed based on slant angle. The slanted

type maximum and minimum response value is included for comparison. Overall, the optimal layout selection process requires a balanced combination of device performance, which includes sensitivity towards applied mechanical strains and figure of merit calculation based on the extracted data.

Table 2. Summary of sensor's frequency and time-domain analysis with different embedded IDT layouts.

IDT layouts	Type/ spacing	Frequency peak (MHz)	IL (dB)	Output signal (μV)
Focused	30°	3.96	-134	39.7
	45°	4.14	-140	43.2
	60°	3.8	-136	41.8
Circular	Spiral	3.92	-139	43.4
	Holographic	3.65	-141	26.9
Slanted	50~100 μm	4.18/1.54	-154/-139	52.7/10.5
Bi-directional	-	3.96	-135	38.7

3. MECHANICAL STRAIN ANALYSIS

For the mechanical strain analysis, initial strain conditions are applied on the sensor placed under no strain to 20,000 $\mu\epsilon$ with 5,000 $\mu\epsilon$ increments. The strain and ambient phenomenon are accounted as static load, while the input voltage signal is a harmonic load. The S-parameter is replaced and represented with root mean squared (RMS) displacements based on COMSOL numerical tool. Mechanical strain is applied in the longitudinal direction, where an increase in strain value will increase the spacing between the IDTs and wave velocity, resulting in changes in wave characteristics. Figure 3 (a-f) indicates the shifts in resonant frequency due to changes in wave velocity and amplitude, which are utilized to execute the sensitivity of each layout towards applied longitudinal mechanical strains. Also, the shift in amplitude is greater with 20,000 $\mu\epsilon$ due to the higher strain applied, which can be another indicator of extreme strain monitoring. Among different layouts, FIDT 45° and spiral show higher sensitivity of 0.4311 ppm/ $\mu\epsilon$ and 0.4478 ppm/ $\mu\epsilon$, associated with a change in frequency from the resonant peak, as listed in Table 3. A focused layout with 45° will be more suitable for jetting or strain detection applications with higher amplitude waves at a specific point. Spiral layout utilization can be expanded by adding multiple output ports, which not only increase the area of detection but also enable efficient sensitivity. Overall, these two layouts along with the slanted, will be integrated to form a 3D shape layout that will enable IDT to sense in multiple directions.

Table 3. Sensitivity of sensor with different layouts towards mechanical strain.

IDT layouts	Type/ spacing	Mechanical strain sensitivity (ppm/με)	
	30°	0.427	
Focused	45°	0.431	
	60°	0.425	
Circular	Spiral	0.447	
	Holographic	0.416	
Slanted	50 ~100 μm	0.411/0.407	
Bi-directional	1	0.260	

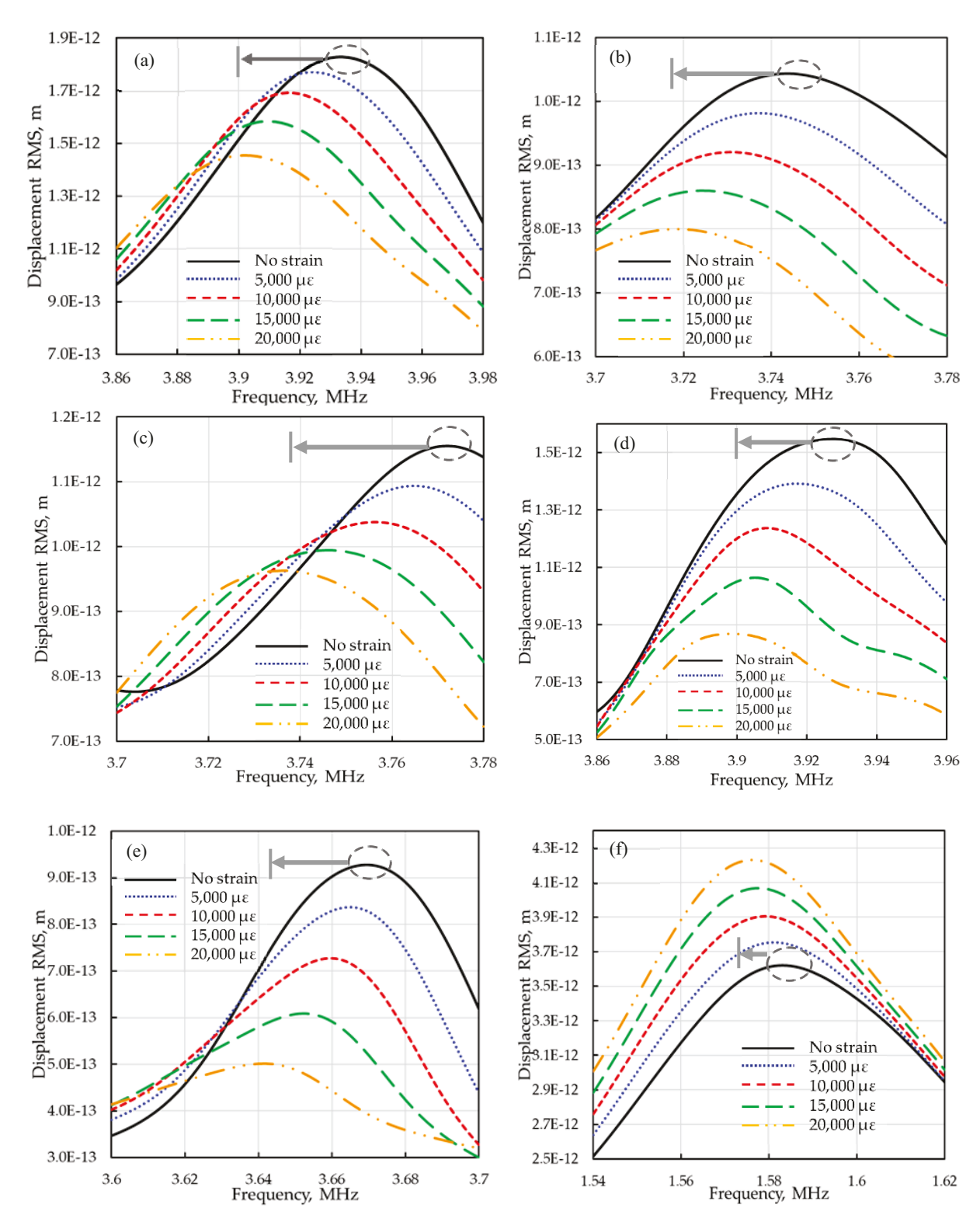


Figure 3. Numerical strain analysis showing a shift in resonant peak as a function of mechanical strain for different IDT layouts: FIDTs (a) 30° , (b) 45° , (c) 60° ; circular pattern (d) spiral, (e) holographic, and (f) slanted with $100 \ \mu m$ spacing.

4. FIGURE OF MERIT: COUPLING COEFFICIENT AND QUALITY FACTOR

Examining the figure of merit, which is a combination of the coupling coefficient (k^2) and quality factor in addition to the sensitivity, would be ideal in the IDT layout selection process, as the electrodes are embedded inside the substrate¹⁷. The k^2 indicates a piezoelectric material's effectiveness in converting an electrical signal into a mechanical wave and vice versa. The quality factor is a dimensionless parameter representing the rate of energy loss relative to the sensor's stored energy. Both the factors are combined as a figure of merit and are calculated based on the expression¹⁸, which involves resonance (f_r) and anti-resonance (f_a) frequency peak from the impedance response derived from S-parameter, as shown in equations (3) and (4),

$$k^{2} (\%) = \frac{\pi}{2} \left(\frac{f_{r}}{f_{a}} \right) \tan \left[\frac{\pi}{2} \left(\frac{f_{a} - f_{r}}{f_{a}} \right) \right] * 100$$
 (3)

$$Q = \left| \frac{f_0}{f_0 - f_r} \right| \tag{4}$$

Table 4. Figure of merit comparison between different IDT layouts.

IDT layouts	Type/ spacing	k ² (%)	Quality factor (Q)	$FOM \\ (Q \times k^2)$
Focused	30°	10.84	24.75	2.683
	45°	13.70	20	2.740
	60°	8.32	31.67	2.633
Circular	Spiral	8.04	32.67	2.628
	Holographic	15.17	18.25	2.769
Slanted	50~100 μm	27.36/ 3.65	11/69.67	3.01/ 2.54

By comparing the simulation data, as listed in Table 4, it is evident that FIDT with 45° degree of arc indicates higher FOM along with sensitivity. However, to expand layout selection into multi-axial mechanical strain measurement with higher sensing area, circular shapes would be the best candidate by implementing multiple output electrodes that can be integrated all together into an antenna. Additionally, a piezoelectric sensor with different electrode layouts embedded inside shows overall better performance than a conventional bi-directional design and can be implemented in respective fields based on the application.

5. CONCLUSION

This paper presents the investigation of wave-based piezoelectric sensor performance with different electrode layouts. The wave characteristics with different embedded electrode layouts are studied in both time and frequency domains. Among different layouts, focused design with 45° degree of arc and spiral design shows a higher sensitivity of 0.431 ppm/ $\mu\epsilon$ and 0.4478 ppm/ $\mu\epsilon$ to the mechanical strains. A FOM is obtained based on the simulated data to illustrate the effectiveness of the layout in addition to the sensitivity. Lastly, a circular layout would be an ideal candidate for sensing mechanical strains in a larger area with multiple output ports. In the future, an integrated IDT design will be developed for sensing multi-axial mechanical strains that can be printed using high-resolution additive manufacturing techniques.

ACKNOWLEDGMENT

This material is based upon work supported by the National Science Foundation under Grant No. 2229155. The opinions, findings, and conclusions, or recommendations expressed are those of the author(s) and do not necessarily reflect the views of the National Science Foundation.

REFERENCES

- [1] Song, S., Wang, Q., Zhou, J. *et al.*, "Design of interdigitated transducers for acoustofluidic applications," Nanotechnology and Precision Engineering, 5(3), 035001 (2022).
- [2] Srinivasaraghavan Govindarajan, R., Rojas-Nastrucci, E., and Kim, D., "Surface Acoustic Wave-Based Flexible Piezocomposite Strain Sensor," Crystals, 11(12), 1576 (2021).
- [3] Aleksandrova, M., and Badarov, D., "Recent Progress in the Topologies of the Surface Acoustic Wave Sensors and the Corresponding Electronic Processing Circuits," Sensors, 22(13), 4917 (2022).
- [4] Mazalan, M. B., Noor, A. M., Wahab, Y. *et al.*, "Current development in interdigital transducer (IDT) surface acoustic wave devices for live cell in vitro studies: A review," Micromachines, 13(1), 30 (2021).
- [5] Sirohi, J., and Chopra, I., "Fundamental understanding of piezoelectric strain sensors," Journal of intelligent material systems and structures, 11(4), 246-257 (2000).
- [6] Rufo, J., Cai, F., Friend, J. *et al.*, "Acoustofluidics for biomedical applications," Nature Reviews Methods Primers, 2(1), 30 (2022).
- [7] Sankaranarayanan, S. K., and Bhethanabotla, V. R., "Design of efficient focused surface acoustic wave devices for potential microfluidic applications," Journal of Applied Physics, 103(6), 064518 (2008).
- [8] Wu, T.-T., Tang, H.-T., Chen, Y.-Y. *et al.*, "Analysis and design of focused interdigital transducers," IEEE transactions on ultrasonics, ferroelectrics, and frequency control, 52(8), 1384-1392 (2005).
- [9] Yatsuda, H., "Design techniques for SAW filters using slanted finger interdigital transducers," IEEE transactions on ultrasonics, ferroelectrics, and frequency control, 44(2), 453-459 (1997).
- [10] Zheng, T., Liu, Y., Xu, C. *et al.*, "Focusing surface acoustic waves assisted electrochemical detector in microfluidics," Electrophoresis, 41(10-11), 860-866 (2020).
- [11] Ziping, W., Xiqiang, X., Lei, Q. *et al.*, "Research on the Progress of Interdigital Transducer (IDT) for Structural Damage Monitoring," Journal of Sensors, 2021, 1-10 (2021).
- [12] Srinivasaraghavan Govindarajan, R., Madiyar, F., and Kim, D., "Flexible Piezoelectric Wave-Based Sensor: Numerical Analysis And Validation," Smart Materials, Adaptive Structures and Intelligent Systems. 86274, V001T05A007.
- [13] Zhang, Q., Han, T., Tang, G. et al., "SAW characteristics of AlN/SiO 2/3C-SiC layered structure with embedded electrodes," IEEE Transactions on Ultrasonics, Ferroelectrics, and Frequency Control, 63(10), 1608-1612 (2016).
- [14] Srinivasaraghavan Govindarajan, R., Stark, T., Sikulskyi, S. *et al.*, [Piezoelectric strain sensor through reverse replication based on two-photon polymerization], SPIE, SS (2022).
- [15] Srinivasaraghavan Govindarajan, R., Xu, X., Sikulskyi, S. *et al.*, "Additive manufacturing of flexible nanocomposite SAW sensor for strain detection," Sensors and Smart Structures Technologies for Civil, Mechanical, and Aerospace Systems 2021. 11591, 115910F.
- [16] Liu, G., Li, Z., Li, X. et al., "Design and experiment of a focused acoustic sorting chip based on TSAW separation mechanism," Microsystem Technologies, 26, 2817-2828 (2020).
- [17] Hao, Z., Park, M., Kim, D. G. *et al.*, "Single Crystalline ScAlN Surface Acoustic Wave Resonators with Large Figure of Merit (Q× k_t²)," 2019 IEEE MTT-S International Microwave Symposium (IMS). 786-789.
- [18] Asseko Ondo, J. C., Blampain, E. J. J., N'Tchayi Mbourou, G. *et al.*, "FEM modeling of the temperature influence on the performance of SAW sensors operating at gigahertz frequency range and at high temperature up to 500 C," Sensors, 20(15), 4166 (2020).